Tran-SET

Transportation Consortium of South-Central States

Solving Emerging Transportation Resiliency, Sustainability, and Economic Challenges through the Use of Innovative Materials and Construction Methods: From Research to Implementation

Modeling Sulfate Attack in Modern Concrete for Building Sustainable and Resilient Infrastructure

Project No. 17CTAM01

Lead University: Texas A&M University

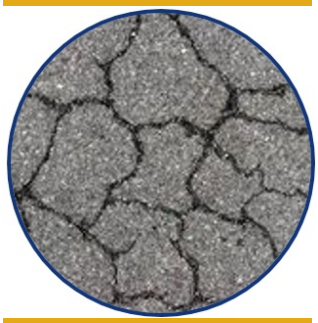

Enhancing Durability and Service Life of Infrastructure

Final Report

October 2018

Disclaimer

The contents of this report reflect the views of the authors, who are responsible for the facts and the accuracy of the information presented herein. This document is disseminated in the interest of information exchange. The report is funded, partially or entirely, by a grant from the U.S. Department of Transportation's University Transportation Centers Program. However, the U.S. Government assumes no liability for the contents or use thereof.

Acknowledgments

We acknowledge the support and direction of the Project Review Committee members, Dr. David Zollinger, Dr. Anol Mukhopadhyay, and Dr. Xiaodan Li, in successfully conducting this research.

TECHNICAL DOCUMENTATION PAGE

1. **Project No.**	**2. Government Accession No.**	**3. Recipient's Catalog No.**
17CTAM01		

4. Title and Subtitle	**5. Report Date**
Modeling Sulfate Attack in Modern Concrete for Building Sustainable and Resilient Infrastructure	Oct. 2018
	6. Performing Organization Code
7. Author(s)	**8. Performing Organization Report No.**
PI: Zachary Grasley https://orcid.org/0000-0002-4246-196X Post-doc: Syeda Rahman https://orcid.org/0000-0002-7111-0333	
9. Performing Organization Name and Address	**10. Work Unit No. (TRAIS)**
Transportation Consortium of South-Central States (Tran-SET) University Transportation Center for Region 6 3319 Patrick F. Taylor Hall, Louisiana State University, Baton Rouge, LA 70803	**11. Contract or Grant No.** 69A3551747106
12. Sponsoring Agency Name and Address	**13. Type of Report and Period Covered**
United States of America Department of Transportation Research and Innovative Technology Administration	Final Research Report May 2017 – May 2018
	14. Sponsoring Agency Code

15. Supplementary Notes

Report uploaded and accessible at: Tran-SET's website (http://transet.lsu.edu/)

16. Abstract

External sulfate attack is a complex phenomenon and is manifested in the form of large expansion, cracking, and spalling depending on the exposure solution and material constituent properties. Several models were developed in the past to demonstrate sulfate attack mechanisms that account for the diffusion of sulfate ions into the porous concrete and the successive deformation triggered by the chemical reaction and precipitation of expansive agents. However, none of these models accounts for the effect of the migration of solvent water from the low solute concentration solution to high solute concentration solution driven by the osmotic pressure. Osmotic pressure is believed to cause spalling and cracking of concrete substrates coated with semipermeable membrane that prohibits diffusion of ions from the surroundings into the porous body. In order to determine the effect of osmotic pressure on the deformation of concrete exposed to sulfate solution, a coupled poromechanical model has been developed. Sensitivity analysis has been performed to investigate the effect of material constituent properties and exposure solution on the osmotic pressure induced damage propensity of concrete. It has been found that concrete surface can exhibit high instantaneous tensile stress developed by the gradient in the salt concentration between the pore solution and external surroundings.

17. Key Words	**18. Distribution Statement**
Sulfate attack, osmotic pressure, poromechanics, early damage	No restrictions.

19. Security Classif. (of this report)	**20. Security Classif. (of this page)**	**21. No. of Pages**	**22. Price**
Unclassified	Unclassified	17	

Form DOT F 1700.7 (8-72) **Reproduction of completed page authorized.**

SI* (MODERN METRIC) CONVERSION FACTORS

APPROXIMATE CONVERSIONS TO SI UNITS

Symbol	When You Know	Multiply By	To Find	Symbol
		LENGTH		
in	inches	25.4	millimeters	mm
ft	feet	0.305	meters	m
yd	yards	0.914	meters	m
mi	miles	1.61	kilometers	km
		AREA		
in^2	square inches	645.2	square millimeters	mm^2
ft^2	square feet	0.093	square meters	m^2
yd^2	square yard	0.836	square meters	m^2
ac	acres	0.405	hectares	ha
mi^2	square miles	2.59	square kilometers	km^2
		VOLUME		
fl oz	fluid ounces	29.57	milliliters	mL
gal	gallons	3.785	liters	L
ft^3	cubic feet	0.028	cubic meters	m^3
yd^3	cubic yards	0.765	cubic meters	m^3
		NOTE: volumes greater than 1000 L shall be shown in m^3		
		MASS		
oz	ounces	28.35	grams	g
lb	pounds	0.454	kilograms	kg
T	short tons (2000 lb)	0.907	megagrams (or "metric ton")	Mg (or "t")
		TEMPERATURE (exact degrees)		
^oF	Fahrenheit	5 (F-32)/9 or (F-32)/1.8	Celsius	^oC
		ILLUMINATION		
fc	foot-candles	10.76	lux	lx
fl	foot-Lamberts	3.426	candela/m^2	cd/m^2
		FORCE and PRESSURE or STRESS		
lbf	poundforce	4.45	newtons	N
lbf/in^2	poundforce per square inch	6.89	kilopascals	kPa

APPROXIMATE CONVERSIONS FROM SI UNITS

Symbol	When You Know	Multiply By	To Find	Symbol
		LENGTH		
mm	millimeters	0.039	inches	in
m	meters	3.28	feet	ft
m	meters	1.09	yards	yd
km	kilometers	0.621	miles	mi
		AREA		
mm^2	square millimeters	0.0016	square inches	in^2
m^2	square meters	10.764	square feet	ft^2
m^2	square meters	1.195	square yards	yd^2
ha	hectares	2.47	acres	ac
km^2	square kilometers	0.386	square miles	mi^2
		VOLUME		
mL	milliliters	0.034	fluid ounces	fl oz
L	liters	0.264	gallons	gal
m^3	cubic meters	35.314	cubic feet	ft^3
m^3	cubic meters	1.307	cubic yards	yd^3
		MASS		
g	grams	0.035	ounces	oz
kg	kilograms	2.202	pounds	lb
Mg (or "t")	megagrams (or "metric ton")	1.103	short tons (2000 lb)	T
		TEMPERATURE (exact degrees)		
^oC	Celsius	1.8C+32	Fahrenheit	^oF
		ILLUMINATION		
lx	lux	0.0929	foot-candles	fc
cd/m^2	candela/m^2	0.2919	foot-Lamberts	fl
		FORCE and PRESSURE or STRESS		
N	newtons	0.225	poundforce	lbf
kPa	kilopascals	0.145	poundforce per square inch	lbf/in^2

TABLE OF CONTENTS

LIST OF FIGURES

ACRONYMS, ABBREVIATIONS, AND SYMBOLS

Ca	Calcium
Fe	Iron
FHWA	Federal Highway Administration
K	Potassium
Mg	Magnesium
$MgSO_4$	Magnesium sulfate
Na	Sodium
Na_2SO_4	Sodium sulfate

a^L	Solvent activity coefficient
b	Biot's coefficient
$\underline{\underline{\varepsilon}}$	Infinitesimal strain tensor
ε_f	Free strain
ε_r	Radial strain component
ε_θ	Tangential strain component
$\in$	Volumetric strain
ϕ	Current Lagrangian porosity
ϕ_0	Initial Lagrangian porosity
φ	Porosity variation
$\underline{\underline{I}}$	Identity tensor
G	Shear modulus of the porous material
K	Bulk modulus of the porous material
K^L	Bulk modulus of the pore liquid
K_s	Bulk modulus of the solid skeleton
η^L	Viscosity of the pore liquid
k	Intrinsic permeability
M	Modulus relating the pore pressure to initial Lagrangian porosity and porosity variation at zero strain
M^L	Molar mass of the solvent water
N	Modulus relating the pore pressure to porosity variation at zero strain
ν	Poisson's ratio of the porous material
p^L	Pore liquid pressure
R	Universal gas constant
ρ^L	Density of the pore liquid
$\underline{\underline{T}}$	Cauchy stress tensor
T_r	Radial stress component
T_θ	Tangential stress component
θ	Temperature
u	Radial deformation

EXECUTIVE SUMMARY

External sulfate attack is known to be one of the most widespread and common forms of chemical degradation of concrete infrastructure and requires extensive rehabilitation within a few years of construction costing millions of dollars every year. Such degradation process is triggered by the diffusion of external sulfate ions through the pore network of concrete located in the geologic environment rich with sulfate ions. The diffused sulfate ions then react with the hydrated and unhydrated cement matrix components and form expansive ettringite. Many experimental investigations have been performed and predictive models have been developed to study the effect of sulfate attack and the resulting expansion. However, none of these studies involve the effect of osmotic pressure on the damage propensity of concrete exposed to sulfate bearing solution. Osmotic pressure is the pressure induced by the differential solute concentration that draws solvent from the low solute concentration to the high solute concentration solution. It is believed to cause spalling and cracking in concrete coated with semipermeable membranes that prohibit ingress of ions from external surroundings to the structure. To test this hypothesis that osmotic pressure plays a role in concrete deformation due to exposure to sulfate solution, a coupled poromechanical model has been developed. This model determines stresses and strains in saturated cylindrical specimens immersed in sulfate solution. For simplicity, the diffusion of solutes into the pore network is not considered and hence the formation of expansive agents is neglected.

It is found that the osmotic pressure can develop high instantaneous tensile stresses at the surface when cylinder is exposed to sulfate solution due to the spatial gradient in the sulfate concentration across the radial position. Sensitivity of osmotic pressure induced stresses and strains to different constituent properties have also been investigated to identify material properties that can mitigate such early damage. Mandel-Cryer effect is also found to play a critical role in stress relaxation and the osmotic pressure induced damage propensity can be exacerbated by certain material properties such as low permeability and high porosity. It is believed that such a mechanistic model incorporating the effect of osmotic suction in concrete deformation will allow engineers to understand the underlying mechanism dictating the damage evolution process by short-term sulfate exposure, where the sulfate ions have not diffused through the pore network to react with the hydrated products and precipitate as expansive agents.

IMPLEMENTATION STATEMENT

In order to disseminate the developed model and research results to the public, students, researchers, and practitioners, a user-friendly software interface is being created for the developed model. With this interface, the user will be able to obtain stress, strain, and pressure outputs for the assigned input parameters.

Workforce Development: The member (post-doctoral researcher) working on this research project developed a new modeling skill specializing in multi-physics, multi-phase material modeling. She also learned poro-mechanics, a relatively new field to the concrete society.

Supporting Outreach Activities: A conference paper was published and a presentation was given at the Tran-SET 2018 conference in New Orleans, Louisiana.

Education: A user interface is currently being built for the developed model that will serve as an educational module for students, researchers, and engineers. Users will be allowed to input parameters including material properties and sulfate solution concentration to observe how the short-term sulfate solution exposure may develop critical stresses and strains in the concrete structure and may lead to damage.

1. INTRODUCTION

According to the nation's existing highway and transit condition and performance report published by the Federal Highway Administration (FHWA), over $35 billion was spent in 2012 in replacing and rehabilitating the existing pavements and bridges *(1)*. Even though the concrete structures were built conforming to the building codes and recommendations, much of the rehabilitation is due to the material deterioration exposed to aggressive environments. Sulfate attack is known to be the most widespread form of chemical degradation of concrete that appears in regions where concrete is exposed to soil or water containing sulfates. External sulfate attack, due to its complicated nature, has led to numerous researches, both experimental and theoretical, Experimental determination of concrete susceptibility to sulfate attack involves long-term immersion of concrete specimens in sulfate solution. While these tests that require months to perform, manifest damage in the form of large expansion, field investigations indicate evidence of high stresses at surface leading to cracks or softening and disintegration of the cement matrix. Moreover, the alternative recommended accelerated tests do not mimic the field conditions. Based on the previously performed experimental studies, the current design code prescribes a maximum allowable limit for the tricalcium aluminate phase in cement to mitigate the problem. This limit prohibits practitioners from using local raw materials and researchers from engineering binders with broad chemical and physical properties. Little data are available for modern materials for which increasing substitution of cement is utilized to reduce energy consumption and environmental emission. In addition, the mechanism and distress type caused by different sulfate solutions containing Na, Mg, Ca, K, and Fe are not fully known. For example, cement with low tricalcium aluminate, as prescribed by the design code to withstand damage caused by the sodium sulfate solution, may prove detrimental when exposed to magnesium sulfate or sulfuric acid *(2)*.

Due to the complex nature of sulfate attack and varied effects caused by different sulfate bearing solutions, extensive studies have been performed and a vast literature is present on the topic *(2-14)*. Several models were developed in the past focusing on the volumetric expansion of concrete *(6)*, crystallization pressure generated by the crystal growth in the pore network *(8)*, and poroelastic damage based on the reactive diffusion model *(14)*. However, none of these models account for the osmotic suction caused by gradient in the salt concentration in the pore solution.

The osmotic suction can be defined as the difference in pressures exerted by solutes on either side of a semi permeable membrane due to spatial gradient in the solute concentration *(15)*. As a result, solvent is drawn out of low solute concentration solution to high solute concentration solution. While, osmotic suction is recognized to initiate damage in organic coatings on concrete substrates in the form of delamination, folding, and blisters *(16)*, its effect on deformation of concrete structures subject to sulfate (more generally to any salt) solution is not known.

2. OBJECTIVES

The primary objective of this work is to develop a coupled poromechanical model and to theoretically test the hypothesis that osmotic suction plays a role in the development of early damage during sulfate attack. In addition, the effect of material constituent properties and exposure solution on the osmotic pressure induced stresses and strains in saturated concrete is also studied. Furthermore, this work demonstrates the importance of incorporating osmotic pressure in developing prospective coupled chemo-poro-elastic diffusion-binding-mechanical models that can accurately predict concrete deformation and damage potential due to short-term sulfate attack.

3. SCOPE

In order to determine the effect of osmotic suction on concrete deformation, the proposed work utilizes poroelasticity *(17)* to develop a coupled linear elastic model that accounts for the difference in pore pressure driven by the spatial gradient in solute concentration. A cylindrical concrete specimen saturated with pure water is assumed to be subjected to sulfate solution of a given concentration. It is assumed that the diffusion of solute in the pore solution is much slower than the diffusion of water molecules so that there is no expansive agent formed in the pore network.

4. METHODOLOGY

For modeling purposes, it is assumed that a cylindrical concrete specimen, completely saturated with pure water, is immersed in a sulfate solution bath with known solute concentration. The pore pressure at the boundary is calculated from the water activity of the solution bath. The concrete specimen is assumed to be coated with a semipermeable membrane such that no solute is diffused into the specimen allowing the transport of solvent only.

4.1. Governing Equations

The governing equations associated with the mass balance and linear momentum balance for an elastic porous material are used. In absence of inertia and body forces, the conservation of linear momentum provides *(18)*:

$$\mathrm{div}\underline{\underline{T}} = 0 \qquad [1]$$

where $\underline{\underline{T}}$ is the externally applied total Cauchy stress tensor that is expressed (for a linearly isotropic material) as:

$$\underline{\underline{T}} = 2G\left[\underline{\underline{\varepsilon}} + \frac{\nu}{1-2\nu}\mathrm{tr}\left(\underline{\underline{\varepsilon}}\right)\underline{\underline{I}}\right] - 3K\,\varepsilon_f\,\underline{\underline{I}} \qquad [2]$$

where:

$\underline{\underline{\varepsilon}}$ = infinitesimal strain tensor,

G = shear modulus of the porous body,

K = bulk modulus of the porous body,

ε_f = free strain,

ν = Poisson's ratio of the porous body, and

$\underline{\underline{I}}$ = identity tensor.

For a poroelastic material with invariant porosity upon pressurization, the free strain, ε_f, can be denoted as *(17,19)*:

$$\varepsilon_f = \frac{b\,p^L}{3K} \qquad [3]$$

where:

p^L = liquid pressure and

b = Biot's coefficient, and can be defined as:

$$b = 1 - \frac{K}{K_s}, \qquad [4]$$

where K_s is bulk modulus of the solid phase comprising the skeleton of the porous body.

The liquid pressure, p^L, can be determined using the liquid continuity equation along with Darcy's law:

$$\frac{\partial\left(\phi\,\rho^L\right)}{\partial t}=\mathrm{div}(\rho^L\frac{k}{\eta^L}\mathrm{grad}p^L) \qquad [5]$$

where:
ρ^L = undeformed density of the liquid phase,
k = intrinsic permeability with dimensions of length squared,
η^L = viscosity of the pore liquid, and
$\phi\,\rho^L$ = the total mass of water per unit initial volume of the porous material with the current Lagrangian porosity, ϕ.

For cylinders with high aspect ratio, the problem simplifies to one dimensional problem on account of symmetry about the longitudinal axis. Moreover, when the specimen is saturated with poorly compressible liquid, such as water, Equation [5] simplifies to:

$$b\frac{\partial \in}{\partial t}+\frac{1}{M}\frac{\partial p^L}{\partial t}=\frac{k}{\eta^L}\frac{1}{r}\frac{\partial}{\partial r}\left(r\frac{\partial}{\partial r}p^L\right) \qquad [6]$$

where:
$\in$ = volumetric strain and
M = modulus relating the pore pressure to initial Lagrangian porosity and porosity variation at zero strain.

The constitutive equation, below, is used in Equation [6]:

$$\varphi=b\in+\frac{p^L}{N} \qquad [7]$$

where N is the modulus relating pore pressure to porosity variation at zero strain. N linearly relates the pore pressure, p^L, to the porosity variation, $\varphi=\phi-\phi_0$, when the volumetric deformation, $\in$ is zero. The modulus, M, is defined as:

$$\frac{1}{M}=\frac{\phi_0}{K^L}+\frac{1}{N} \qquad [8]$$

where:
K^L = the bulk modulus of the pore liquid and
ϕ_0 = the initial Lagrangian porosity.

For long concrete cylinders (with length/diameter > 2), on account of the symmetry all three shear strains and stresses are zero. The non-zero stresses along the radial and tangential directions, T_r and T_θ satisfy the equilibrium Equation [1] as:

$$\frac{dT_r}{dr}+\frac{T_r-T_\theta}{r}=0 \qquad [9]$$

In addition, the radial and tangential strains can be expressed as:

$$\varepsilon_r=\frac{du}{dr} \text{ and } \varepsilon_\theta=\frac{u}{r} \qquad [10]$$

where u is the radial displacement.

Substitution of Equations [2], [3], and [10] in [9], gives the conservation of linear momentum for cylindrical coordinate system:

$$\frac{d}{dr}\left(\frac{1}{r}\frac{d\left(r\,u\right)}{dr}\right)=\left(1+\nu\right)\frac{b}{3K}\frac{dp^L}{dr} \qquad [11]$$

Since, both the governing Equations [6] and [11], have two variables, u and p^L, these two equations need to be solved simultaneously to capture the coupled poromechanical interaction of the porous body and the pore solution.

4.2. Boundary Conditions

Initially the specimen is assumed to be saturated with pure water. The initial condition associated with this assumption is:

$$p^L{}_{(r,t=0)}=0 \qquad [12]$$

There exists no flow condition at the center due to axial symmetry, therefore,

$$\left(\frac{\partial p^L}{\partial r}\right)_{r=0,t}=0 \qquad [13]$$

The boundary pressure at the surface is determined using the following expression:

$$p^L{}_{r=D/2,t}=-\rho^L\frac{R\theta}{M^L}\ln\left(a^L\right) \qquad [14]$$

where:

D = the diameter of the cylinder,

R = the universal gas constant,

θ = the temperature,

M^L = the molar mass of the solvent water, and

a^L = activity coefficient of the solvent water. The water activity is defined as the reduction in vapor pressure due to the presence of solutes only.

The mechanical initial and boundary conditions are as follows:

$$u_{(r,t=0)} = 0 \qquad [15]$$

$$\left(\frac{\partial u}{\partial r}\right)_{r=0,t} = 0, \text{ due to axial symmetry, and} \qquad [16]$$

$$T_{r=D/2,t} = 0. \qquad [17]$$

as the specimen is subject to zero stress at the boundary.

Figure 1 shows the model geometry along with the osmotic pressure applied at the boundary. Coupled Equations [6] and [11] are solved simultaneously to determine the unknowns, u and p^L for the boundary conditions specified by [12] to [17] and using the NDSolve function in Mathematica.

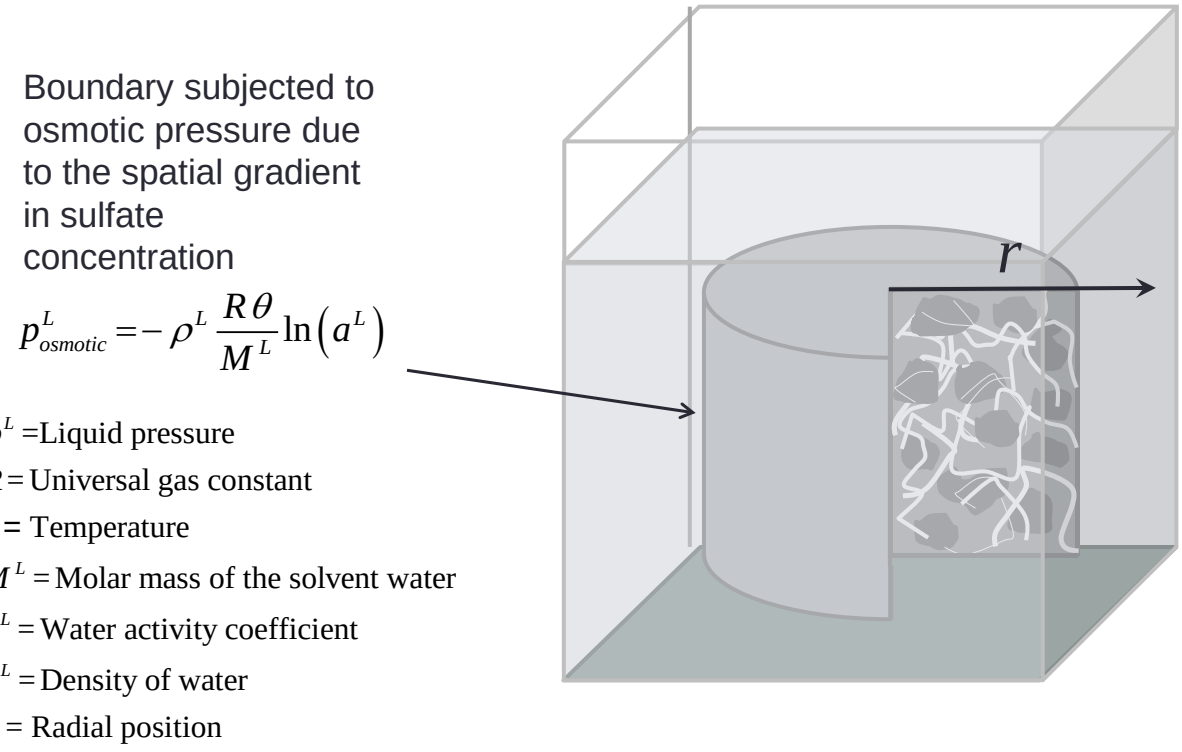

Figure 1. Geometry of the water saturated specimen immersed in sulfate solution.

5. RESULTS

The simulated pore pressure, bulk strain, tangential stresses for a 6 in diameter cylinder are plotted in Figure 2. The following materials properties are assumed: $k = 1\times10^{-19}\,\mathrm{m}^2$, $K_s = 25.4\times10^3\,\mathrm{MPa}, \text{and}\, K = 11.1\times10^3\,\mathrm{MPa}$ with a porosity of 0.2. The concrete specimen is assumed to be immersed in 3 mol/kg Na_2SO_4 solution. The corresponding water activity coefficient is obtained to be 0.9 *(20)*, which according to equation [14], gives the boundary pressure of $-13.24\,\mathrm{MPa}$. In this study, as the specimen is assumed to be saturated with pure water and contains no solute in the pore solution, a sudden exposure to the salt solution creates significant spatial gradient in the solute concentration. As a result, high osmotic suction is developed at the boundary which draws solvent molecules (water) from the specimen center to surface. Since, concrete is a weakly permeable material, water takes a long time to drain to the surface to equilibrate with the boundary pressure (Figure 2 (a)). As a result, boundary contracts more than the center that exhibits higher pressure than the surface (Figure 2 (b)). This differential strain across the radial position develops instantaneous high tensile tangential stresses at the boundary as shown in Figure 2 (c). This high stress has a potential to create micro-cracks at the concrete surface, which may exacerbate the problem when the expansive agents are precipitated in the pore network accompanied by the diffusion of sulfate ions and may lead to peeling or flaking of materials. Due to the coupled poromechanical action, right before the pressure at the center equilibrates with the pressure at the boundary; it rises above the initial value and takes longer to equilibrate. The strain compatibility, which requires the entire body to contract due to the suction applied at the surface, squeezes the center and increases the pressure above the initial value. This phenomenon, which is demonstrated to exacerbate the freezing deformation of concrete due to big aggregates with poor permeability *(21)*, is popularly known as the Mandel-Cryer effect *(22)* in geomechanics and petroleum engineering.

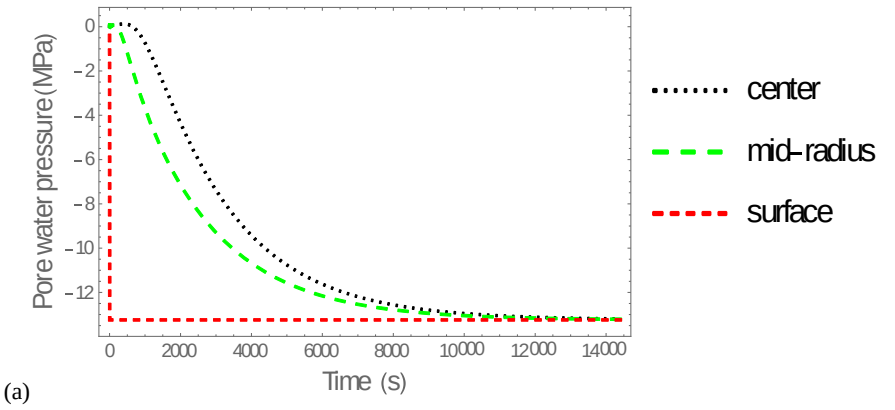

(a)

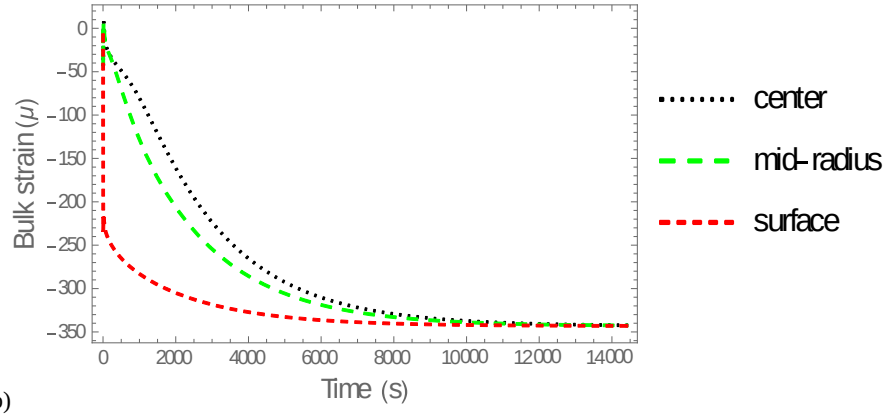

(b)

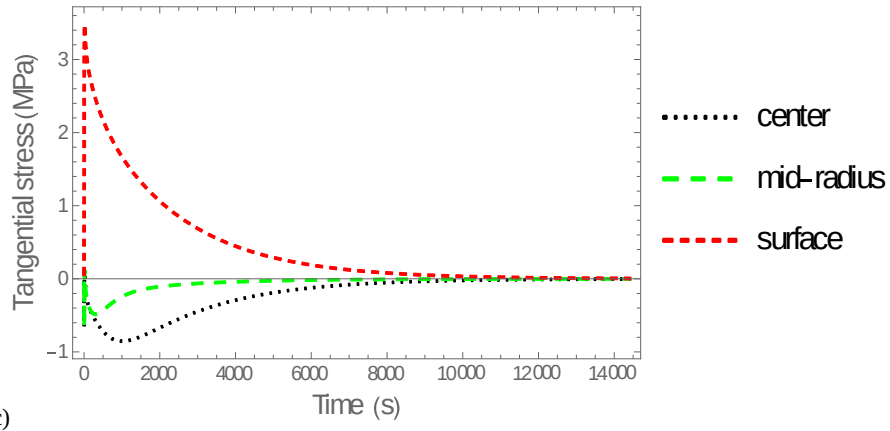

(c)

Figure 2. (a) Osmotic pore pressure, (b) bulk strain, and (c) tangential stress developed in a cylindrical concrete specimen exposed to 6% Na_2SO_4 solution.

For the modeling purposes and to demonstrate the effect of osmotic pressure, it is assumed that the specimen is initially saturated with pure water. This assumption is an extreme hypothetical scenario, which is necessary to create a significant spatial differential in the solute concentration and to develop high pressure gradient between the concrete specimen and the surrounding solution bath. In the field, because of the dissolved ions in the pore solution, the osmotic suction gradient will be much lower with very low stresses and strains than the values reported here. In the event that pore solution has higher concentration than the surrounding bath of the sulfate solution, pore pressure gradient will develop and water will migrate toward the surrounding solution. Because of this pore pressure gradient, differential strain will develop across the specimen which in turn will induce tensile stresses. Regardless of the direction of water migration, as long as the spatial gradient exists in the pore network, water will move from the high solute concentration region to low solute concentration region, and short-term high stresses will be exhibited.

5.1. Sensitivity Analysis

The following sections investigate the effect of salt solution, concrete permeability, porosity, and compressibility on the osmotic pressure induced stresses and strains.

5.1.1. Effect of Sulfate Exposure

When sulfates with different cations are dissolved in water, its activity is lowered significantly based on the type and concentration of the dissolved ions. For instance, saturated $MgSO_4$ solution can reduce the vapor pressure of water significantly and can provide water activity as low as 0.1 *(23)*. In order to demonstrate how sulfates with different cations can affect osmotic pressure induced stresses and strains in concrete, two different water activities are considered. The simulated results are shown in Figure 3. It has been seen that very low water activity, either due to high concentration of sulfate ions or sulfates with different cations, can increase the osmotic suction at the surface significantly and develop significant contraction at the center. As a result, a very high tensile stress can be exhibited at the surface leading to spalling or cracking well before the solute reacts with the cement matrix and precipitates in the pore network. This high stress take a long time to relax and increases material susceptibility to damage for several hours.

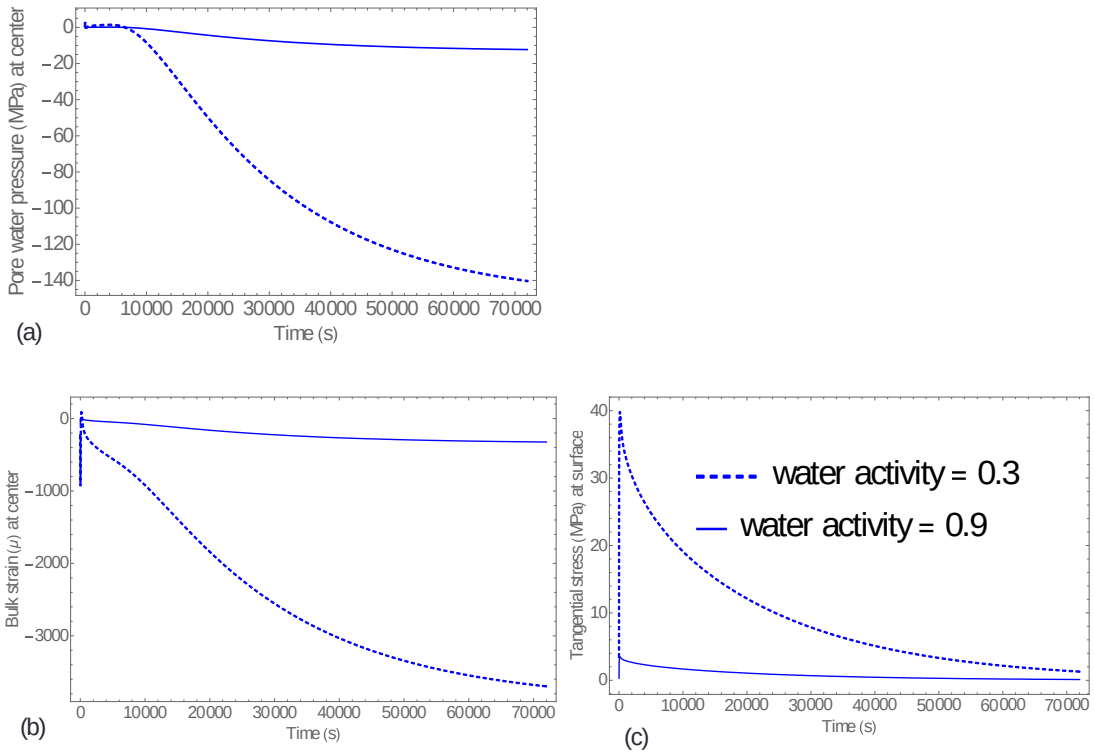

Figure 3. Effect of exposure to sulfate solution on the simulated (a) pore pressure at the center, (b) bulk strain at the center, and (c) tangential stresses at the surface.

5.1.2. Effect of Permeability, Porosity, and Compressibility

Figure 4 shows simulations for three different concrete cylinders with different permeability $k = 10^{-18}$, $k = 10^{-19}$, and $k = 10^{-20}$. Simulated results show that low permeability does not affect the magnitude of peak stress developed instantly. However, it reduces the rate at which the pressure at the center equilibrates with the boundary. Lower the permeability, higher the time to relax the pore pressure at the center. Consequently, the Mandel-Cryer effect is extended for a prolonged period. This extended Mandel-Cryer effect sustains high-strain gradient across the specimen radial location for a long time, and retards stress relaxation at the surface significantly.

The bulk modulus of the porous concrete is related to the porosity through the relation, $K = K_s\left(1-\phi_0\right)^2$. To show the effect of porosity and compressibility, three different concrete specimens are considered with three different values for porosity, $\phi_0 = 0.1$, $\phi_0 = 0.2$, and $\phi_0 = 0.3$, and three different values for skeleton bulk modulus, $K_s = 13.7\times10^3$ MPa, $K_s = 17.3\times10^3$ MPa, and $K_s = 22.7\times10^3$ MPa. It has been revealed from Figure 5 that high porosity and high skeleton bulk modulus increase the magnitude of instantaneous peak tensile stress at the surface. Such characteristics also exacerbate the damage propensity by intensifying the Mandel-Cryer effect and delaying the stress relaxation. Due to the extended Mande-Cryer effect, the center contracts at a slower rate than the initial rate, maintaining the strain gradient

for an extended period. As a result, high-porosity concrete exhibits higher peak tensile stress for an elongated period and is more prone to osmotic suction induced early damage than a low-porosity concrete.

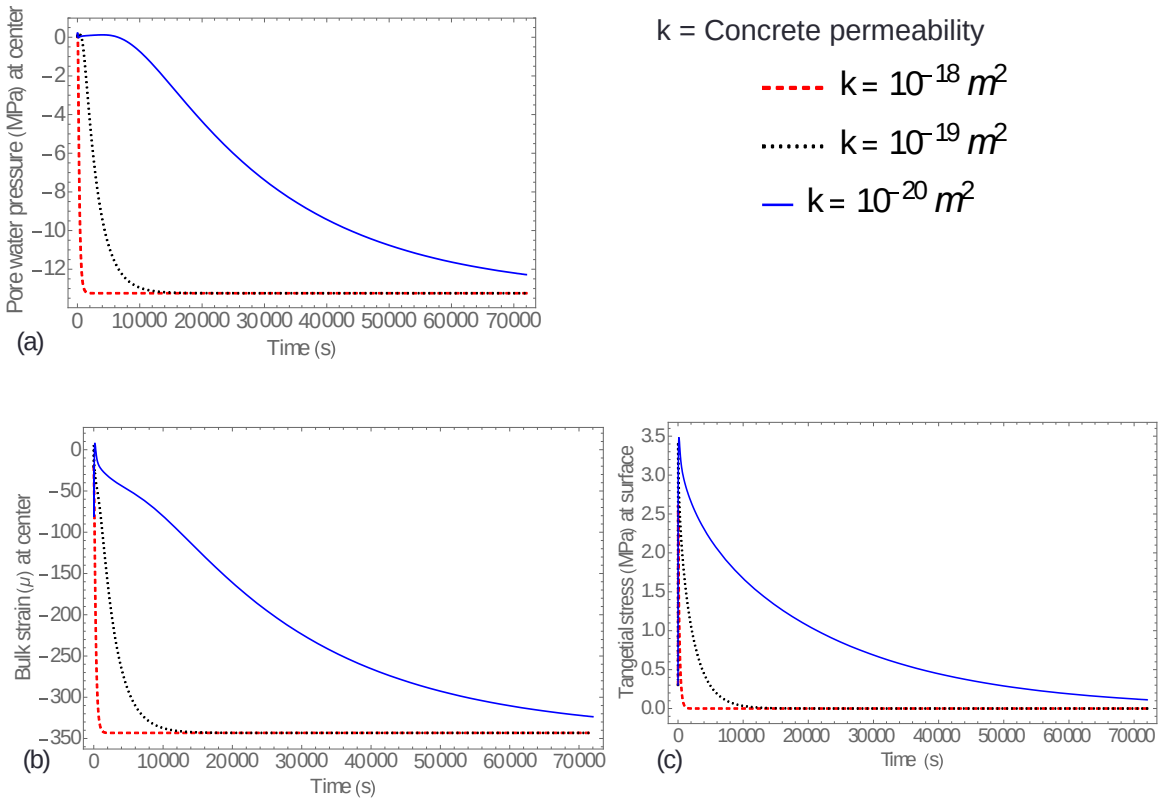

Figure 4. Effect of permeability on the simulated (a) pore pressure at the center, (b) bulk strain at the center, and (c) tangential stresses at the surface.

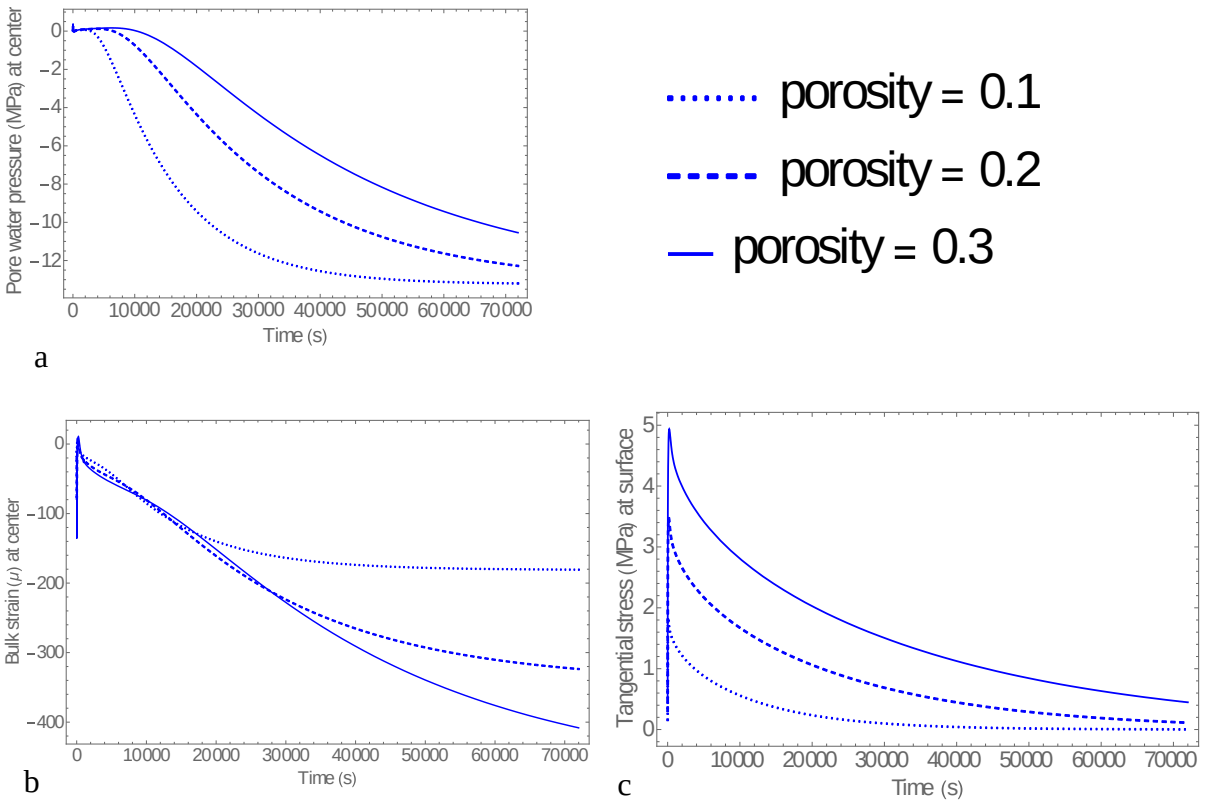

Figure 5. Effect of porosity on the simulated (a) pore pressure at the center, (b) bulk strain at the center, and (c) tangential stresses at the surface.

6. CONCLUSIONS

From the simulated results, it is found that differential strain caused by high pressure gradient can exert instantaneous tensile tangential stress at the concrete boundary when it is exposed to sulfate solution. This pressure gradient can be attributed to osmotic suction caused by the spatial gradient in solute concentration, which draws liquid water (solvent only) from low solute concentration to high solute concentration. As a result, high differential in the volumetric strain can be observed which in turn can cause tensile tangential stress at the boundary. When this tensile stress exceeds the tensile strength of the material, it can create spalling or flaking at the surface. This stress may also serve as weak spots for future cracking or spalling when the long-term diffusion of sulfate ions into the pore network may eventually cause reaction and subsequent precipitation in the pore network leading to expansion.

It has been also found that the intensity of the osmotic suction induced stresses and strains depend on the sulfate bearing cations and solute concentration. High solute concentration or sulfate bearing cations that lower water activity significantly can develop high stress at the surface for a prolonged period. Low permeability and high porosity may also exacerbate the osmotic pressure induced damage propensity in concrete by exposing the material surface to high stress. In this case, both parameters intensify the Mande-Cryer effect which delays stress relaxation for several hours. This Mandel-Cryer effect occurs due to the coupled poro-mechanical interaction between the solid skeleton of the porous body and the pore solution.

7. RECOMMENDATIONS

In light of the simulated results, it is expected that the osmotic suction plays an important role in the deformation of concrete exposed to sulfate solution, and needs to be incorporated in the diffusion-binding-mechanical model to accurately predict concrete deformation. The present work captures the short-term diffusion of the solvent only and does not include the diffusion of salts to pore solution and the subsequent reaction with the hydrated product and crystallization. It is believed that the incorporation of osmotic pressure in a coupled chemo-poro-elastic diffusion-binding-mechanical model will help engineers understand the mechanism of concrete deformation (both expansion due to crystallization and spalling at the surface) exposed to sulfate solution. In addition, experimental research needs to be performed to validate the proposed hypothesis and the modeled results.

REFERENCES

1. *2015 Status of the Nation's Highways, Bridges, and Transit: Conditions & Performance*. [1/30/2017]; Available from: https://www.fhwa.dot.gov/policy/2015cpr/es.cfm#6h.

2. Santhanam, M., M.D. Cohen, and J. Olek, *Sulfate attack research — whither now?* Cement and Concrete Research, 2001. **31**(6): p. 845-851.

3. Santhanam, M., M.D. Cohen, and J. Olek, *Mechanism of sulfate attack: A fresh look: Part 1: Summary of experimental results.* Cement and Concrete Research, 2002. **32**(6): p. 915-921.

4. Santhanam, M., M.D. Cohen, and J. Olek, *Mechanism of sulfate attack: a fresh look: Part 2. Proposed mechanisms.* Cement and Concrete Research, 2003. **33**(3): p. 341-346.

5. Neville, A., *The confused world of sulfate attack on concrete.* Cement and Concrete Research, 2004. **34**(8): p. 1275-1296.

6. Tixier, R. and B. Mobasher, *Modeling of Damage in Cement-Based Materials Subjected to External Sulfate Attack. I: Formulation.* Journal of Materials in Civil Engineering, 2003. **15**(4): p. 305-313.

7. Ferraris, C., et al., *Developing a More Rapid Test to Assess Sulfate Resistance of Hydraulic Cements.* J Res Natl Inst Stand Technol, 2005. **110**(5): p. 529-40.

8. Bary, B., *Simplified coupled chemo-mechanical modeling of cement pastes behavior subjected to combined leaching and external sulfate attack.* International Journal for Numerical and Analytical Methods in Geomechanics, 2008. **32**(14): p. 1791-1816.

9. Drimalas, T., et al., *Laboratory and Field Evaluations of External Sulfate Attack in Concrete*. 2011, University of Texas at Austin, Center for Transportation Research (CTR): Austin, Tx.

10. Pignatelli, R., C. Comi, and P.J.M. Monteiro, *A coupled mechanical and chemical damage model for concrete affected by alkali–silica reaction.* Cement and Concrete Research, 2013. **53**: p. 196-210.

11. Ikumi, T., et al., *Alternative methodology to consider damage and expansions in external sulfate attack modeling.* Cement and Concrete Research, 2014. **63**: p. 105-116.

12. Cefis, N. and C. Comi, *Damage modelling in concrete subject to sulfate attack.* Frattura e Integrita Strutturale, 2014(29): p. 222-229.

13. Cefis, N. and C. Comi, *Multi-Phase Modelling of Concrete Affected by Sulfate Attack.* Applied Mechanics and Materials, 2015. **784**: p. 86-94.

14. Cefis, N. and C. Comi, *Chemo-mechanical modelling of the external sulfate attack in concrete.* Cement and Concrete Research, 2017. **93**: p. 57-70.

15. Grasley, Z.C. and K.R. Rajagopal, *Revisiting total, matric, and osmotic suction in partially saturated geomaterials.* Zeitschrift für angewandte Mathematik und Physik, 2011. **63**(2): p. 373-394.

16. Günter, M. and H.K. Hilsdorf, *Stresses Due to Physical and Chemical Actions in Polymer Coatings on a Concrete Substrate*, in *Adhesion between polymers and concrete / Adhésion entre polymères et béton: Bonding · Protection · Repair / Revêtement · Protection · Réparation*, H.R. Sasse, Editor. 1986, Springer US: Boston, MA. p. 8-21.

17. Biot, M.A., *General Theory of Three-Dimensional Consolidation.* Journal of Applied Physics, 1941. **12**(2): p. 155-164.

18. Timoshenko, S. and J.N. Goodier, *Theory of Elasticity*. 1951, New York: McGraw-Hill. 416-420.

19. Coussy, O., *Poromechanics*. 2004, West Sussex: John Wily & Sons, Ltd.

20. Guendouzi, M.E., A. Mounir, and A. Dinane, *Water activity, osmotic and activity coefficients of aqueous solutions of Li_2SO_4, Na_2SO_4, K_2SO^4, $(NH_4)_2SO_4$, $MgSO_4$, $MnSO_4$, $NiSO_4$, $CuSO_4$, and $ZnSO_4$ at T=298.15K.* The Journal of Chemical Thermodynamics, 2003. **35**(2): p. 209-220.

21. Rahman, S. and Z. Grasley, *A poromechanical model of freezing concrete to elucidate damage mechanisms associated with substandard aggregates.* Cement and Concrete Research, 2014. **55**: p. 88-101.

22. Wang, H., *Theory of linear poroelasticity with applications to geomechanics and hydrogeology*. 2000, New Jersey: Princeton University Press.

23. Jones, E.G. and C.H. Lineweaver, *Using the phase diagram of liquid water to search for life.* Australian Journal of Earth Sciences, 2012. **59**(2): p. 253-262.